Current Applied Physics 9 (2009) 1062–1066

Contents lists available at ScienceDirect

Current Applied Physics

journal homepage: www.elsevier.com/locate/cap

# Synthesis protocol influence on aqueous magnetic fluid properties

M. Răcuciu

*Lucian Blaga University, Faculty of Science, Dr. I. Ratiu Street, No. 5–7, Sibiu 550024, Romania*

ARTICLE INFO

*Article history:*
Received 17 July 2008
Received in revised form 17 November 2008
Accepted 3 December 2008
Available online 10 December 2008

*PACS:*
47.65.Cb
81.16.Be
96.15.Pf

*Keywords:*
Magnetic nanoparticles
Different preparation protocol
Rheological properties
Magnetic properties
TEM
IR spectra

ABSTRACT

Magnetic colloids containing superparamagnetic $Fe_3O_4$ nanoparticles have been prepared by co-precipitation method. Three samples of citric acid coated magnetic colloids containing magnetic nanoparticles (ultra-fine particles of $Fe_3O_4$) have been obtained following three different preparation protocols. Physical tests have been performed on these samples of the magnetic colloids prepared by us (consisting mainly of $Fe_3O_4$ ultra-fine particles stabilized with citric acid ($C_6H_8O_7$) and immersed in water), in order to reveal their microstructural and rheological features. Transmission electron microscopy (TEM) and magnetic measurements were the investigation methods used for the assessing of the magnetic nanoparticles size. The dimensional distribution of the ferrophase physical diameter was comparatively presented using the box-plot statistical method. Infrared absorption spectra have been recorded aiming to get some information on the magnetic fluid composition.

© 2008 Elsevier B.V. All rights reserved.

## 1. Introduction

The interest in magnetic fluid preparation arises from the fact that they exhibit rheological properties of fluids from the dynamic viewpoint, but can be controlled directly by the application of a magnetic field – which can not happen with any natural fluid. Magnetic fluids are stable colloidal dispersions of ultra-fine (mostly) spherical ferro- or ferri-magnetic particles, such as magnetite ($Fe_3O_4$) or maghemite ($\gamma$-$Fe_2O_3$), in a nonmagnetic liquid carrier [1], which may be chosen to conform to a particular application. The dispersion of the ferrophase is ensured by coating the nanoparticles with adequate surfactant (able to assure steric or electrostatic stabilization) [2].

Thus, the attraction forces between magnetic dipoles as well as the Van der Waals forces can be balanced while the tendency of precipitation in gravitational or magnetic field could also be compensated – the magnetic colloid stability being assured [3]. The magnetic properties of magnetite, that make it a desirable component of magnetic fluids, are derived from its crystal structure. Magnetite crystallizes in the inverse spinel structure [4], consisting of iron oxide ions in a cubic close-packed arrangement. The 1/4 of the octahedral holes are occupied by $Fe^{2+}$ ions while the $Fe^{3+}$ ions are equally divided between 1/8 of the tetrahedral holes and 1/4 of the octahedral holes; electron spins of $Fe^{3+}$ ions in octahedral holes are aligned anti-parallel to those in tetrahedral holes while the $Fe^{2+}$ ions tend to align their spins parallel with those of $Fe^{3+}$ ions in adjacent octahedral sites, leading to a net magnetization.

The properties of magnetic fluids have been intensively studied due to their multiple applications [5,6], in both technical and life sciences. Magnetite nanoparticles with superparamagnetic properties have great potential to achieve convenient properties for biomedical applications due to their biocompatibility, it is known that the human body contains around 3 g Fe within the proteins like ferritin, hemosiderin, transferritin and hemoglobin and, also that the iron oxides are gradually recycled naturally.

Various synthesis methods, adequate for magnetic nanoparticle preparation have been described in literature, like chemical co-precipitation [7,8], sonochemical reactions [9], sol–gel [10], microwave heating [11], mechanochemical [12], micelle microemulsion [13,14] or solvothermal reduction [15]. Compared to other methods, chemical routes have often been found as most convenient methods used for the production of high quality magnetic nanoparticles.

In the present work, we describe the differences evidenced in the properties of three samples of biocompatible magnetic fluid prepared by different protocols, using citric acid for magnetite stabilization.

*E-mail address:* mracuciu@yahoo.com

1567-1739/$ - see front matter © 2008 Elsevier B.V. All rights reserved.
doi:10.1016/j.cap.2008.12.003

## 2. Materials and methods

Three samples of magnetic fluid containing magnetic nanoparticles (mostly ultra-fine particles of $Fe_3O_4$) coated with citric acid have been obtained following three different preparation protocols [16–18]. The first magnetic fluid sample (**A**) was prepared by mixing FeCl3 and FeSO4 in the presence of excess ammonia, according to [16]. Ferrophase was precipitated by dissolving 5.6 g $FeSO_4 \cdot 7H_2O$ and 10.8 g $FeCl_3 \cdot 6H_2O$ in 300 ml deionized water, heating up to 80 °C and adding 200 ml of 25% $NH_4OH$ under vigorous and continuous stirring for 60 min.

In the ferrophase synthesis process, the first step was hydrolysis of the iron salts, following the equations:

$$2FeCl_3 + 6H_2O \rightarrow 6Cl^- + 6H^+ + 2Fe(OH)_3 \quad (1)$$

$$FeSO_4 + 2H_2O \rightarrow SO_4^{2-} + 2H^+ + Fe(OH)_2 \quad (2)$$

The $NH_4^+$ cations combined with the anions resulted on the iron salts hydrolysis:

$$8NH_4^+ + 6Cl^- + SO_4^{2-} \rightarrow 6NH_4Cl + (NH_4)_2SO_4 \quad (3)$$

The process of the $Fe_3O_4$ nucleation achieved following the reaction:

$$2Fe(OH)_3 + Fe(OH)_2 + 8OH^- + 8H^+ \rightarrow Fe_3O_4 + 12H_2O \quad (4)$$

After the washing of magnetite – up to neutral pH – it was stabilized with 5 g of citric acid in 10 ml deionized water at the temperature of 90 °C.

For the second sample of magnetic fluid (**B**), aqueous solutions of 4.16 g $FeCl_2 \cdot 4H_2O$ and, respectively 10.44 g $FeCl_3 \cdot 6H_2O$ in 380 ml deionized water, were heated at 80 °C and mixed under vigorous and continuous stirring with 40 ml of 25% $NH_4OH$ as precipitant agent [17].

In the ferrophase synthesis process the first step was hydrolysis of the iron (II) and iron (III) salts, following the Eq. (1) and:

$$2FeCl_2 + 4H_2O \rightarrow 4Cl^- + 4H^+ + 2Fe(OH)_2 \quad (5)$$

Further, the $NH_4^+$ ions combined with the $Cl^-$ anions resulted from the iron salts hydrolysis:

$$NH_4^+ + Cl^- \rightarrow NH_4Cl \quad (6)$$

The process of the $Fe_3O_4$ nucleation occurred following the reaction:

$$2Fe(OH)_3 + Fe(OH)_2 + 2OH^- + 2H^+ \rightarrow Fe_3O_4 + 6H_2O \quad (7)$$

Finally, 5 g of citric acid in 10 ml deionized water was added to the well-washed ferrophase and the temperature was raised to 90 °C under continuous stirring for 60 min.

The third sample (**C**) was synthesized via a controlled chemical precipitation approach, at room temperature under acidic conditions as described by Berger *et al.* [18]. Acidic solutions of ferric and ferrous salts were prepared in 2 M HCl instead of deionized water since the acidic conditions prevent the formation of iron hydroxides. We have mixed 1.0 ml of 2 M stock $FeCl_2$ solution and 4.0 ml of 1 M stock $FeCl_3$ solution under continuous magnetic stirring for 60 min by adding 50 ml of 0.7 M aqueous $NH_3$ solution. The synthesis based on co-precipitation of iron (II) and iron (III) ions in an aqueous ammonia solution, resulting in $Fe_3O_4$ precipitation, following the equation:

$$2FeCl_3 + FeCl_2 + 8NH_3 + 4H_2O \rightarrow Fe_3O_4 + 8NH_4Cl \quad (8)$$

The iron oxide particles obtained this way, were non-magnetically mixed with 6 ml citric acid 25% solution. All three types of fluid magnetic systems are assumed to contain mainly magnetite as ferrophase – though maghemite presence is not excluded due to the unavoidable oxidization processes – colloidal particle dispersion being ensured by the same type of stabilization – the electrostatic repulsion that occurs due to the charges of citrate ions adsorbed on the magnetic particle surface.

Physical tests have been performed on the three magnetic fluids prepared by, in order to reveal their microstructural and rheological features. The magnetic fluid density (picnometric method), viscosity (capillary method) and surface tension (stalagmometric method) have been measured using standard methods. The pH measurements were carried out with universal indicative paper (Merck). Transmission electron microscopy (TEM) was the main investigation method for the assessing of the physical size of the magnetic nanoparticles. TEM photographs were provided by a TESLA device (sample deposition of collodion sheet after $10^4$ dilutions). The dimensional distribution of the ferrophase physical diameter was comparatively presented using the box-plot statistical method [19]. Measurements of magnetization and magnetic susceptibility were performed revealing the suitability of the aqueous magnetic fluid for magnetic carrier utilization, following the Gouy method at constant normal temperature. Infrared spectra have been recorded aiming to get some information on the magnetic fluid composition. The IR investigation was carried out using a Perkin–Elmer 580 device for the scanning of the magnetic fluid dispersion in KBr after previous thermal treatment at 100 °C up to constant weight. All reagents were high purity substances from Merck Company.

## 3. Results and discussion

The aqueous magnetic fluid samples prepared as described above were dark-brown colloids that exhibited positive magnetic behavior in the presence of a permanent magnet. In Fig. 1, TEM image of the magnetic nanoparticles coated with citric acid is shown.

Image analysis was accomplished upon about 1000 particles per every magnetic fluid sample (Fig. 1). The results of all TEM image measurements on the physical diameter value ranged between 10.65 and 11.45 nm as presented in Table 1, exhibiting mostly

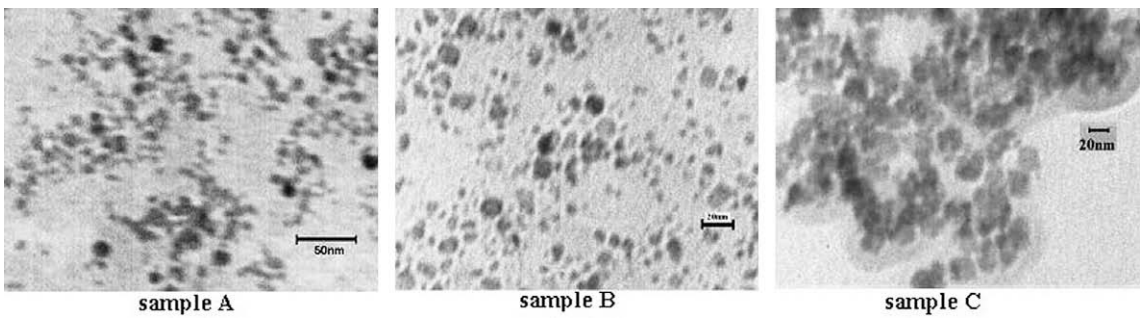


**Fig. 1.** TEM image for citric acid coated magnetic fluid samples, synthesized by three different protocols.

**Table 1**
The physical properties, volume fraction data and mean physical diameter of magnetic nanoparticles.

| Magnetic fluid sample | Φ (%) | Density (kg/m$^3$) | Surface tension ($\times 10^{-3}$ N/m) | Viscosity ($\times 10^{-3}$ kg/ms) | pH | $a_{TEM}$ (nm) |
|---|---|---|---|---|---|---|
| **A** | 4.7 | 1081.57 | 71.18 | 1.78 | 6.0 | 10.7 |
| **B** | 4.0 | 1030.64 | 72.48 | 1.45 | 6.5 | 10.6 |
| **C** | 5.0 | 1088.26 | 76.24 | 2.77 | 6.5 | 11.4 |

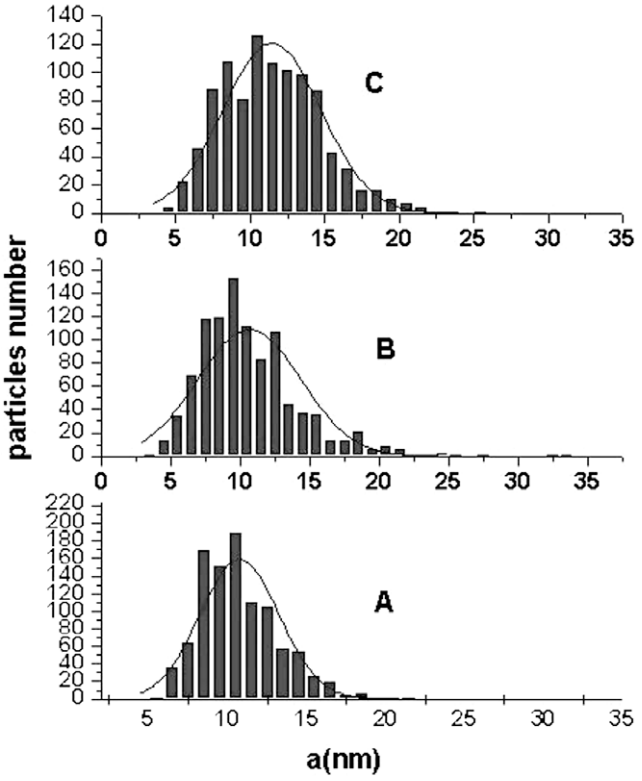


**Fig. 2.** Histograms for the analyzed magnetic fluids – "a" being the physical diameter.

spherical shape. Some large aggregates and particle chains have been also observed.

Also, the results of the physical properties investigations as well as the volume fraction, Φ, of ferrophase in the magnetic fluid samples are presented in Table 1. The average values calculated following ten repetitions of every measurement are given. The highest values of physical properties analyzed in this study, were revealed for C sample, synthesized at room temperature (Fig. 2).

As already know the control on the particle size and size distribution is strongly dependent on the particularities of the preparation protocol. The method involves co-precipitation from $Fe^{2+}$ and $Fe^{3+}$ aqueous salt solutions by addition of a base – ammonium hydroxide, sodium hydroxide, etc. – usually a thigh temperatures but not compulsory. Co-precipitation consists of two processes: nucleation (formation of centers of crystallization) and particle growth. The relative rates of these two processes determine the size and polydispersity of iron oxides particles. Polydispersed colloids are obtained as a result of simultaneous formation of new nuclei and growth of the earlier formed particles. Less size dispersed colloids are formed when the rate of nucleation is high and the rate of particles growth is low, this situation corresponding to a rapid addition and a vigorous mixing of reagents. Slow addition of reagents in the co-precipitation reaction leads to the formation of bigger nuclei. An increase in temperature (in the range 20–100 °C) significantly accelerates formation of ferrite particles. Variation of the pH value of the reacting solution also results into different size of precipitated particles. Regarding the three preparation protocols applied by us the rapid addition of reagents was assured in all cases but the pH of the reaction medium varied considerably as well as the reaction temperature.

The histograms of particle size were transformed into rectangular boxes in order to accomplish comparative analysis of the magnetic fluid samples. In Fig. 3 the box-plot diagram is presented for comparative discussions of dimensional distributions of the three biocompatible magnetic fluid samples.

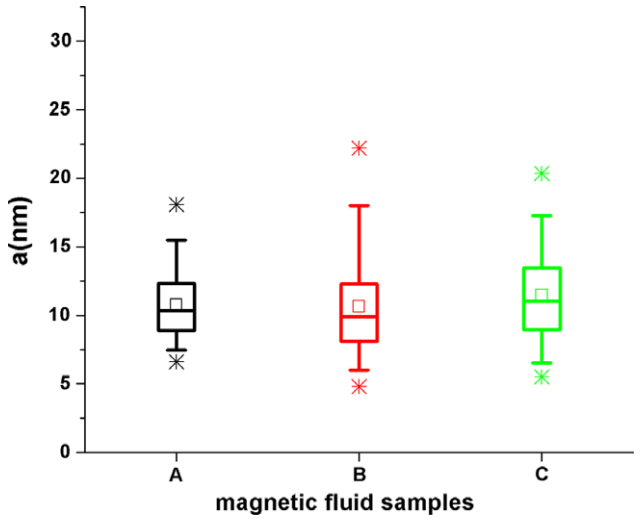


**Fig. 3.** The box-plot representation of physical diameter distribution. In the box-plot representation the point marked within the box length represents the average dimension of magnetic nanoparticles while the points drawn exteriorly represent exceptionally small or large values of particle physical diameter ("a").

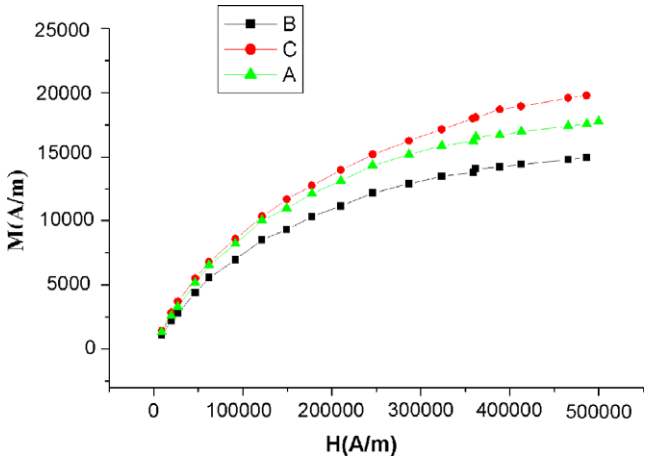


**Fig. 4.** Magnetization curves of magnetic fluid samples.

**Table 2**
The dimensional analysis and magnetic properties data.

| Magnetic fluid sample | $\Phi_M$ (%) | $a_{TEM}$ (nm) | $a_M$ (nm) | $a_{layer}$ (nm) | $M_S$ (kA/m) | $\chi_0$ |
|---|---|---|---|---|---|---|
| **A** | 4.3 | 10.7 | 5.6 | 2.5 | 21.08 | 0.097 |
| **B** | 3.5 | 10.6 | 5.7 | 2.4 | 17.25 | 0.082 |
| **C** | 4.7 | 11.4 | 5.6 | 2.9 | 23.00 | 0.099 |

One can see that the box corresponding to sample **A**, synthesized utilizing excess ammonia, is the narrowest (4.8 nm of box length). In comparison to this sample the magnetic fluids B and C have larger box length values and higher exceptional diameter values especially for sample **B** (22.0 nm) but also for sample **C** (20.8 nm) in comparison to 18.0 nm for sample **A**). The relatively small values of the box edges as well as of the relative small value of the median confirm that the ferrophase size of the magnetic fluid samples is convenient for biological uses.

Magnetization curves are presented in Fig. 4. Using these experimental data and considering the *Langevin* equation at high field, the saturation magnetization values were obtained from magnetization (M) versus 1/H curves, by extrapolating to 1/H = 0, while the initial susceptibility values $\chi_0$ were determined from slope of the magnetization (M) versus magnetic filed (H) curves at low field. The results are presented in Table 2. The magnetic susceptibility versus magnetic field dependences is presented in Fig. 5.

Using magnetic measurements data, the average sizes of magnetic diameter ($a_M$) can be calculated according to *Langevin's* equation, follows:

$$a_M^3 = \frac{18k_BT}{\pi\mu_0 M_b \cdot M_s}\left(\frac{dM}{dH}\right)_{H\to 0} \quad (9)$$

where $a_M$ is the magnetic particle diameter, $k_B$ is Boltzmann's constant, $T$ is the absolute temperature, $M_s$ is the saturation magnetization of the sample and $\mu_0$ is the vacuum magnetic permeability.

Accordingly to Eq. (1) assuming a spherical particle shape and $M_b$ value of bulk magnetite ($0.48\ 10^6$ A/m) [1] we obtained for average magnetic diameter ($a_M$) of nanoparticles for magnetic fluid samples analyzed in this study, the values presented in Table 2.

We can see that the smallest value of the physical diameter was revealed for the magnetic fluid sample synthesized following *Goodarzi* protocol [17], while the high magnetization value was obtained for the magnetic fluid sample synthesized at room temperature. The differences evidenced between $a_{TEM}$ values and $a_M$ values, can be assigned to the size of the surfactant shell of the magnetite core, the surfactant layer being often considered as a magnetically dead coating, which can affect the uniformity or magnitude of magnetization due to quenching of surface moments [20].

Further analysis was carried out by means of IR spectra. Fig. 6 shows the IR absorption recordings. Citric acid (Fig. 7) is a weak organic acid found, naturally, in citrus fruits. It is a natural preservative and also, is recognized as safe for use in foods by all major national and international food regulatory agencies. It is naturally present in almost all forms of life, the excess citric acid being readily metabolized and eliminated from the body.

Non-significant differences between the IR spectra, for these three magnetic fluid samples, were noticed (Fig. 6). The IR spectrum (4000–300 $cm^{-1}$) of the citric acid coated magnetite dispersed in KBr revealed: (i) the large and intense band from 3200 to 3400 $cm^{-1}$ corresponding to the symmetrical and asymmetrical stretchings of OH group confirms the presence of non-dissociated OH groups of the citric acid and water traces; (ii) the intense band at 1600 $cm^{-1}$ may be assigned to the symmetric stretching of CO from COOH group, revealing the binding of citric acid radicals to

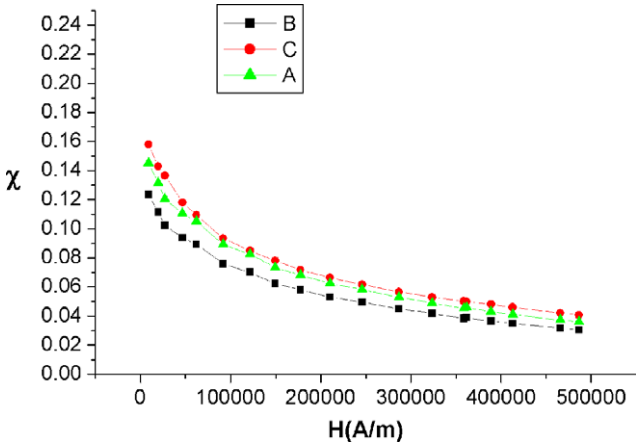


**Fig. 5.** Magnetic susceptibility curves of magnetic fluid samples.

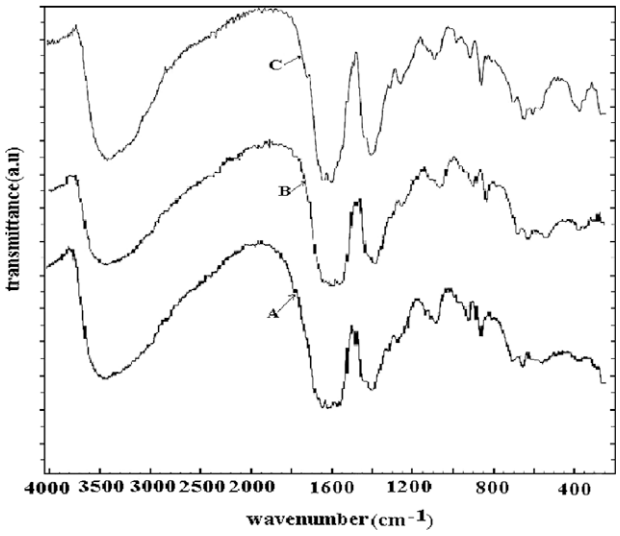


**Fig. 6.** IR spectra of the analyzed magnetic fluid samples stabilized with citric acid.

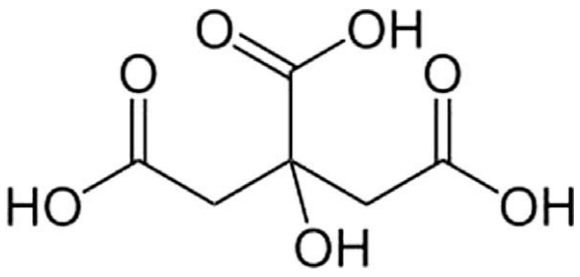


**Fig. 7.** Structural formula of citric acid ($C_6H_8O_7$).

the magnetite surface; (iii) the neighbor band at 1400 $cm^{-1}$ to the asymmetric stretching of CO from COOH group can be assigned; (iv) the low-intensity bands between 400 and 600 $cm^{-1}$ can be associated with the stretching and torsional vibration modes of the magnetite.

Thus, we can say that the citric acid binds chemically to the magnetite surface by carboxylate chemisorption and citrate ions are formed. The chemical adsorption is able to assure electrostatic stabilization of the interaction forces preventing the agglomeration tendency of the magnetic nanoparticles.

## 4. Conclusions

In this study, the physical properties of three samples of water magnetic fluids synthesized by different protocols, all based on iron oxides stabilized with citric acid, were comparatively discussed leading to the evidencing of the most convenient features related to the stability and biological application suitability.

So, the highest density, viscosity, surface tension and volume fraction were evidenced for the magnetic fluid sample **C** synthesized in acidic conditions at room temperature while the physical diameter measurements provided the narrowest distribution and smaller values of the ferrophase physical diameter corresponding to the magnetic fluid sample A synthesized utilizing excess ammonia though sample **C** seems to be also convenient.

## References

[1] R.E. Rosensweig, Ferrohydrodynamics, Cambridge University Press, Cambridge, 1985.
[2] E. Tombácz, A. Majzik, Zs. Horvát, E. Illés, Romanian Reports in Physics 58 (3) (2006) 281.
[3] C. Scherer, A.M. Figueiredo Neto, Braz. J. Phys. 35 (3a) (2005) 718.
[4] B.G. Hyde, S. Andersson, Inorganic Crystal Structures, Wiley, New York, 1989.
[5] S. Odenbach, J. Phys. Condens. Matter (2006) 18.
[6] G. Matei, A. Airinei, D.-E. Creanga, Acta Physica Polonica A 109 (3) (2006) 405.
[7] M. Timko, A. Dzarova, P. Kop cansky, V. Zavisova, M. Koneracka, J. Kovac, A. Sprincova, M. Vlaclavikova, L. Jvanicova, I. Vavra, Acta Physica Polonica A 113 (1) (2008) 573.
[8] S. Sun, H. Zeng, Journal of Applied Chemical Society 124 (2002) 8204.
[9] R. Vijayakumar, Y. Koltypin, I. Felner, A. Gedanken, Material Science and Engineering A 286 (2000) 101.
[10] R. Kornak, D. Niznansky, K. Haimann, W. Tylus, K. Maruszewski, Materials Science-Poland 23 (1) (2005) 87.
[11] W.W. Wang, Y.J. Zhu, M.L. Ruan, Journal of Nanoparticle Research 9 (2007) 419.
[12] C.R. Lin, Y.M. Chu, S.C. Wang, Materials Letters 60 (4) (2006) 447.
[13] M. Gotić, T. Jurkin, S. Musić, Colloid and Polymer Science 285 (7) (2007) 793.
[14] M. Zhang, B.L. Cushing, C.J. O'Connor, Nanotechnology 19 (2008) 085601.
[15] Y. Hou, J. Yu, S. Gao, J. Mater. Chem. 13 (2003) 1983.
[16] C. Cotae, S. Istrate, M. Agop, Gh. Calugaru, The Annals of the University "Dunarea de Jos" of Galati IIXVI (XXI) (1998) 29.
[17] A. Goodarzi, Y. Sahoo, M.T. Swihart, P.N. Prasad, Mat. Res. Soc. Symp. Proc. 789 (2004) N6.6.1.
[18] P. Berger, N.B. Adelman, K.J. Beckman, D.J. Campbell, A.B. Ellis, G.C. Lisensky, J. Chem. Educ. 76 (1999) 943.
[19] D. Creanga, C. Cotae, Indian J. Pure Appl. Phys. 34 (12) (1996) 957.
[20] R. Kaiser, G. Miskolczy, J. Appl. Phys. 41 (1970) 1064.